NASA Contractor Report 165689

INSTABILITY AND TRANSITION IN ROTATING DISK FLOW

Mujeeb R. Malik

SYSTEMS AND APPLIED SCIENCES CORPORATION
17 Research Drive
Hampton, Virginia 23666

Contract NAS1-15604
March 1981

National Aeronautics and
Space Administration

Langley Research Center
Hampton, Virginia 23665

TABLE OF CONTENTS

	PAGE
SUMMARY	ii
SECTION 1 - INTRODUCTION	1
SECTION 2 - THEORETICAL ANALYSIS	4
SECTION 3 - NUMERICAL METHOD	8
SECTION 4 - TRANSITION PREDICTION USING THE e^N METHOD	9
SECTION 5 - RESULTS AND DISCUSSION	10
SECTION 6 - CONCLUSIONS	16
REFERENCES	18
FIGURE CAPTIONS	22

SUMMARY

The stability of three-dimensional rotating disk flow is investigated, including the effects of Coriolis forces and streamline curvature. The numerical results show that the critical Reynolds number for establishment of stationary vortex flow is $R_C = 287$. These vortices spiral outwards at an angle of about 11.2° and transition to turbulence occurs when their total amplification is about e^{11}. It is shown that our analysis gives growth rates that compare much better with the available experimental results than do results obtained using the Orr-Sommerfeld equation. The experimental results tend to support the numerical prediction that the number of stationary vortices varies directly with the Reynolds number. Our calculations also indicate the existence of weakly unstable propagating (Type II) modes at low Reynolds numbers ($R_C \approx 49$).

1. INTRODUCTION

The prediction of transition in three-dimensional boundary layers [1-3] is a subject of both fundamental and practical importance in fluid mechanics. Practical interest in the subject centers on the design of laminar flow control (LFC) wings that promise significant improvement in airplane fuel efficiency. At present, the most useful tool for transition prediction in such flows is the so-called e^N method [4]. Hefner and Bushnell [5] and Malik and Orszag [6] show that the exponent N (called the N factor) is of the order 7-11 when transition occurs on LFC swept wings.

The instability mechanism exhibited in the leading edge region of a swept wing is similar to that found in the boundary layer on a rotating disk, since both have mean cross-flow profiles with inflection points. More details on the similarities between the two flows is given in Ref. [7]. The rotating disk flow is amenable to stability analysis in view of von Karman's exact steady solution [8] of the Navier-Stokes equations free of boundary-layer assumptions.

Using hot wire techniques, Smith [9] observed that sinusoidal disturbances appear in a rotating disk boundary layer at sufficiently large Reynolds number. About 32 oscillations were observed within a disk rotation period and analysis indicated that the disturbances propagate at an angle of about 14° relative to the outward drawn radius (where the direction of disk rotation defines positive angles). Later, in a remarkable study using the china-clay technique, Gregory et al [10] observed

about 30 vortices over the disk spiraling outwards at an angle of about 14° (that is, their normals make an angle of about 14° with the outward drawn radius). These vortices, which appeared stationary relative to the rotating frame of the disk, were first observed at a Reynolds number $R_c \approx 430$ [where R is defined after (10) below]. Transition to turbulence occurred at $R_T \approx 530$. The stationary vortex flow established due to a rotating disk has later been studied by several investigators [11-13]. There exists, among these studies, considerable controversy over the value of the critical Reynolds number which in our view can be attributed to the measurement techniques used. There is also some confusion over the number of stationary vortices. Fedorov et al [13], using visual (Napthalene) and acoustic techniques, observed 27-30 vortices at Reynolds numbers $R \geq 387$. However, at low Reynolds numbers, they observed only 14-16 vortices with normals lying at an angle of about 20°.

Stuart [10] analyzed the linear, inviscid stability of rotating disk flow. However, the neglect of viscosity resulted in the prediction of 113-140 vortices over the disk which is about four times larger than the observed value. Brown [14] extended Stuart's work to the viscous case by applying the Orr-Sommerfeld equation to disk flow. Using temporal instability theory, Brown found $R_c \approx 178$, which is much less than the observed value. Recently, Cebeci and Stewartson [3] solved the Orr-Sommerfeld equation for rotating disk profiles using spatial stability theory and found $R_c \approx 176$. They also suggested that wave packets propagate in three dimensional flows in such a way

that $d\alpha/d\beta$ is real. Using this condition Cebeci and Stewartson correlated transition using the e^N method and found the N factor at transition ($R_T \approx 510$) to be about 20 which is much higher than that found for LFC wings ([5],[6]). Bushnell (private communication) argues that a higher N factor may be required for transition in disk flow than on LFC wings because the boundary layer is rotating with the disk while the external disturbances in the surroundings are not. Consequently, there is no direct coupling between the external disturbances and the instability waves in the rotating disk boundary layer.

The Orr-Sommerfeld stability equation neglects the effects of Coriolis forces, streamwise curvature, and nonparallel flow. In Ekman layer flow, Lilly [15] has shown that the Coriolis force has a significant effect on stability at low Reynolds numbers. Lilly showed that the critical Reynolds number for appearance of stationary vortices is higher ($R_C \approx 115$) when the Coriolis force is included in the analysis than when it is neglected ($R_C \approx 85$). In addition to the stationary vortices, he showed the existence of another (Type II) instability caused by the Coriolis force at much lower Reynolds numbers. Such an instability mechanism was also observed in the Ekman layer experiments of Faller and Kaylor [16] and Tatro and Mollo-Christensen [17]. The Ekman layer and the rotating disk are similar in that both are three-dimensional layer flows in which rotation plays a significant role. Lilly's results suggest that the inclusion of the Coriolis force in the stability analysis of rotating disk flow may also lead to a higher critical Reynolds

number for stationary vortices which is in better agreement with observations.

In this paper we present a stability analysis of rotating disk flow in which the effects of Coriolis force and streamline curvature are included. The resulting sixth-order system is solved numerically by a Chebyshev spectral method [18,19]. We also follow the evolution of the disturbance modes using the envelope method [1,6] and calculate the N factor at transition. The work of Kobayashi et al [12], which appeared during the final stages of the present study, also includes the effects of the Coriolis force and streamline curvature. We will comment on this work in Sec. 6.

2. THEORETICAL ANALYSIS

Consider an infinite plane rotating about its axis with angular velocity Ω. We take cylindrical coordinates r^*,θ,z^* with $z^* = 0$ being the plane of the disk and assume the fluid to lie in the half-space $z^*>0$. Let $\bar{p}$, $\bar{u}$, $\bar{v}$, $\bar{w}$, denote the steady state values of pressure and velocity in the r^*,θ,z^* directions, respectively, in the rotating coordinate frame. Von Karman's exact solution [8] of the Navier-Stokes equations for steady laminar rotating disk flow is obtained by setting

$$\bar{u} = r^*\Omega F(z),\ \bar{v} = r^*\Omega G(z),\ \bar{w} = \sqrt{\nu\Omega}H(z),\ \bar{p} = \rho\nu\Omega p(z), \quad (1)$$

where $z = z^*\sqrt{\Omega/\nu}$. The Navier-Stokes equations reduce to the following equations for F,G,H and P:

$$F^2 - (G+1)^2 + F'H - F'' = 0 \quad (2)$$

$$2F(G+1) + G'H - G'' = 0 \quad (3)$$

$$P' + HH' - H'' = 0 \tag{4}$$

$$2F + H' = 0 \tag{5}$$

where the prime denotes differentiation with respect to z. The boundary conditions are

$$F = 0, \quad G = 0, \quad H = 0 \quad (z = 0) \tag{6}$$

$$F = 0, \quad G = -1 \quad (z \to \infty)$$

Now we study the evolution of infinitesimal small disturbances imposed on the steady flow governed by Eqs. (1) - (5). Let r_e^* be the radial location near which the analysis is to be made. Using $r_e^* \Omega$ as the reference velocity, $\delta^* = \sqrt{\nu/\Omega}$ as the reference length, and $\rho r_e^2 \Omega^2$ as the reference pressure, the instantaneous nondimensional velocities u,v,w and pressure p can be written as

$$u(r,\theta,z,t) = \frac{r}{R} F(z) + \tilde{u}(r,\theta,z,t) \tag{7}$$

$$v(r,\theta,z,t) = \frac{r}{R} G(z) + \tilde{v}(r,\theta,x,t) \tag{8}$$

$$w(r,\theta,z,t) = \frac{1}{R} H(z) + \tilde{w}(r,\theta,z,t) \tag{9}$$

$$p(r,\theta,z,t) = \frac{1}{R^2} P(z) + \tilde{p}(r,\theta,z,t) \tag{10}$$

Here the nondimensional radius is $r = r^*\sqrt{\Omega/\nu}$, the Reynolds number is $R = r_e^* \sqrt{\Omega/\nu}$, and r_e^* corresponds to $r = R$.

Substituting Eqs. (7) - (10) in the Navier-Stokes equations and linearizing with respect to the perturbations gives:

$$\frac{\partial\tilde{u}}{\partial t} + \frac{r}{R} F \frac{\partial\tilde{u}}{\partial r} + \frac{G}{R} \frac{\partial\tilde{u}}{\partial\theta} + \frac{H}{R} \frac{\partial\tilde{u}}{\partial z} + \frac{F}{R} \tilde{u} - \frac{2}{R} (G+1) \tilde{v} + \frac{r}{R} F' \tilde{w} \tag{11}$$

$$= \frac{\partial\tilde{p}}{r} + \frac{1}{R} \left[\frac{\partial^2\tilde{u}}{\partial r^2} + \frac{1}{r^2} \frac{\partial^2\tilde{u}}{\partial\theta^2} + \frac{\partial^2\tilde{u}}{\partial z^2} + \frac{1}{r} \frac{\partial\tilde{u}}{\partial r} - \frac{2}{r^2} \frac{\partial\tilde{v}}{\partial\theta} - \frac{\tilde{u}}{r^2}\right]$$

$$\frac{\partial\tilde{v}}{\partial t} + \frac{r}{R} F \frac{\partial\tilde{v}}{\partial r} + \frac{G}{R} \frac{\partial\tilde{v}}{\partial\theta} + \frac{H}{R} \frac{\partial\tilde{v}}{\partial z} + \frac{F}{R} \tilde{v} + \frac{2}{R} (G+1)\, \tilde{u} + \frac{r}{R} G'\tilde{w} \qquad (12)$$

$$= - \frac{1}{r} \frac{\partial\tilde{p}}{\partial\theta} + \frac{1}{R} \left[\frac{\partial^2\tilde{v}}{\partial r^2} + \frac{1}{r^2} \frac{\partial^2\tilde{v}}{\partial\theta^2} + \frac{\partial^2\tilde{v}}{\partial z^2} + \frac{1}{r} \frac{\partial\tilde{v}}{\partial r} + \frac{2}{r^2} \frac{\partial\tilde{u}}{\partial\theta} - \frac{\tilde{v}}{r^2}\right]$$

$$\frac{\partial\tilde{w}}{\partial t} + \frac{r}{R} F \frac{\partial\tilde{w}}{\partial r} + \frac{G}{R} \frac{\partial\tilde{w}}{\partial\theta} + \frac{H}{R} \frac{\partial\tilde{w}}{\partial z} + \frac{H'}{R} \tilde{w} \qquad (13)$$

$$= - \frac{\partial\tilde{p}}{\partial z} + \frac{1}{R} \left[\frac{\partial^2\tilde{w}}{\partial r^2} + \frac{1}{r^2} \frac{\partial^2\tilde{w}}{\partial\theta^2} + \frac{\partial^2\tilde{w}}{\partial z^2} + \frac{1}{r} \frac{\partial\tilde{w}}{\partial r}\right]$$

$$\frac{\partial\tilde{u}}{\partial r} + \frac{1}{r} \frac{\partial\tilde{v}}{\partial\theta} + \frac{\partial\tilde{w}}{\partial z} + \frac{\tilde{u}}{r} = 0 \qquad (14)$$

The boundary conditions are that $\tilde{u},\tilde{v}$, and $\tilde{w}$ vanish at $z = 0,\infty$.

For $R>>1$, the system (11) - (14) may be consistently approximated by replacing factors of r by R and neglecting terms of order R^{-2} and smaller. The replacement of r by R at this stage of the calculation implies that we neglect some nonparallel flow effects. The neglect of terms of order R^{-2} and smaller has little effect on the results discussed below, as we verified by computations in which they were included.

Replacing factors of r by R in (11) - (14) gives a set of equations that are separable in r,θ,t so that the perturbation quantities may be assumed to have the form

$$(\tilde{u},\tilde{v},\tilde{w},\tilde{p}) = (f(z),h(z),\phi(z),\pi(z))e^{i(\alpha r+\beta R\theta-\omega t)} \qquad (15)$$

With this assumption, Eqs. (11) - (14) become (not yet dropping terms of order R^{-2})

$$i(\alpha F+\beta G-\omega)f+F'\phi + i\alpha\pi = \frac{1}{R} [f''-\lambda^2 f - Ff + 2(G+1)h - Hf'] + \frac{1}{R^2} [i\alpha f - 2i\,\beta\, h] - \frac{1}{R^3}\, f \qquad (16)$$

$$i(\alpha F + \beta G-\omega)h + G\phi + i\beta\pi = \frac{1}{R}\,[h''-\lambda^2 h-Fh-2(G+1)f-Hh'] \qquad (17)$$
$$+ \frac{1}{R^2}\,[i\alpha h + 2i\,\beta\, f] - \frac{1}{R^3}\,h$$

$$i(\alpha F + \beta G-\omega)\,\phi + \pi' = \frac{1}{R}\,[\phi''-\lambda^2\phi-H\phi'-H'\phi] + \frac{i}{R^2}\,\alpha\,\phi \qquad (18)$$

$$(i\alpha+\frac{1}{R})f + i\beta h + \phi' = 0 \qquad (19)$$

where $\lambda^2 = \alpha^2 + \beta^2$.

Eliminating π from (16) - (18) by means of (19) gives, neglecting terms of order R^{-2} and smaller,

$$\frac{1}{R}\,[i(D^2-\lambda^2)\,(D^2-\bar{\lambda}^2) + R(\alpha F+\beta G-\omega)\,(D^2-\bar{\lambda}^2) - R(\bar{\alpha}F''+\beta G'')-iHD(D^2-\bar{\lambda}^2)$$
$$- iH'\,(D^2-\bar{\lambda}^2) - iFD^2]\phi+\frac{1}{R}[(G+1)D + 2G']\,\eta = 0 \qquad (20)$$

$$\frac{1}{R}\,[2(G+1)D-iR(\alpha G'-\beta F')]\,\phi+\frac{1}{R}[i(D^2-\lambda^2) + R(\alpha F+\beta G-\omega) - iHD - iF]\eta = 0 \qquad (21)$$

and where $D = d/dz$, $\bar{\alpha}=\alpha-i/R$, $\bar{\lambda}^2 = \alpha\bar{\alpha}+\beta^2$ and $\eta=\alpha h - \beta f$ is proportional to the z-component of the perturbation vorticity. The final result (20) - (21) is a consistent set of stability equations valid to order R^{-1}.

The boundary conditions for the sixth order system (20) - (21) are

$$\phi(0) = \phi'(0) = \eta(0) = 0\ ,\ \phi(\infty) = \phi'(\infty) = \eta(\infty) = 0 \qquad (22)$$

Note that if the Coriolis force and streamline curvature effects are neglected, the above system reduces to the fourth-order Orr-Sommerfeld equation;

$$[i(D^2-\lambda^2)^2 + R(\alpha F+\beta G-\omega)\,(D^2-\lambda^2) - R(\alpha F''+\beta G'')]\phi = 0 \qquad (23)$$

In Sec. 6, we report numerical results for both the sixth order system (20) - (21) and the fourth order equation (23) in order to study the effect of Coriolis force and streamline curvature terms on the stability of flow due to a rotating disk.

3. NUMERICAL METHOD

We solve the Orr-Sommerfeld Equation (23) using the computer code SALLY [1] that employs a spectral method based on Chebyshev polynomials [18-19]. Here we extend the method to solve the sixth order system (20) - (22).

The boundary layer coordinate z, $0 \leq z < \infty$ is mapped into the finite interval $-1 \leq \xi < 1$ by the algebraic mapping

$$\xi = 2 \frac{z}{z+L} - 1 \tag{24}$$

where L is a scale parameter chosen to optimize the distribution of points in ξ. Then $\phi(z)$ and $\eta(z)$ are approximated as the finite Chebyshev polynomial series

$$\phi(z) = \sum_{n=0}^{M} a_n T_n(\xi) \tag{25}$$

$$\eta(z) = \sum_{n=0}^{M} b_n T_n(\xi) \tag{26}$$

Substituting (25), (26), in (20) - (22) and collocating [19] at the discrete points $\xi_j = \cos \pi_j/M$ $(0 \leq j \leq M)$ gives the algebraic eigenvalue problem,

$$A \begin{matrix} a_n \\ b_n \end{matrix} = \omega B \begin{matrix} a_n \\ b_n \end{matrix} \tag{27}$$

where A and B are 2(M+1) x 2(M+1) matrices. The eigenvalue problem (27) is solved globally (if a guess for an eigenvalue is not available) by a generalized QR algorithm or locally (if a good guess is available) by inverse Rayleigh iteration [20]. The resulting scheme is very efficient and accurate. In the present calculations the optimum value of the scaling parameter L was found to be about 1.8. In most of the calculations reported below, M = 34 so 35 Chebyshev polynomials were used.

The accuracy of the method was tested in several ways. First, the number of retained polynomials, M + 1 was varied to check the accuracy of the eigenvalues and eigenfunctions. Then, calculations were made for the stability of Ekman flow. Comparisons were made with the results obtained by Lilly [15] for R = 65, 110, 150, 300 and 500 with good agreement.

For rotating disk flow, the global method gives only one unstable eigenvalue [Im(ω)>0] for R $\gtrsim$ 150 that is insensitive to M. However, spurious unstable modes appear for lower R which are discarded as unphysical because they are very insensitive to M.

4. TRANSITION PREDICTION USING THE e^N METHOD

In three-dimensional flow, the dispersion relation is given by the complex relation

$$\omega = \omega(\alpha,\beta) \tag{28}$$

where α,β, and ω are, in general, complex. Therefore, there are four arbitrary real parameters among α,β, and ω. There are several ways [6] to remove this arbitrariness. In the present study we

employ the envelope method [1]. Here the four conditions are obtained by using temporal stability theory [in which $Im(\alpha) = Im(\beta) = 0$] and by maximizing $Im(\omega)$ with respect to α,β at fixed $Re(\omega)$. The N factor is then given by

$$N = \int_{s_C}^{s_T} \frac{Im(\omega)}{\left| R_e(\vec{v}_g) \right|} \, ds \tag{29}$$

where $\vec{v}_g = (\omega_\alpha, \omega_\beta)$ is the (complex) group velocity and s is the arc length along the curve whose tangent is the real part of the group velocity. Noting that

$$ds = \frac{dR}{Re(\omega_\alpha)} \sqrt{(Re(\omega_\alpha))^2 + (Re(\omega_\beta))^2} = \frac{dR}{Re(\omega_\alpha)} \left| Re(\vec{v}_g) \right| .$$

Eq. (29) can be written as

$$N = \int_{R_C}^{R_T} \frac{Im(\omega)}{Re(\omega_\alpha)} \, dR \tag{30}$$

Here the subscripts C and T indicate critical (linearly unstable) and onset of transition, respectively.

5. RESULTS AND DISCUSSION

Critical and Transition Reynolds Numbers

Some of the available experimental data for critical and transition Reynolds numbers are given in Table 1. It is apparent that there is considerable variation of the observed critical and transition points. We believe that the variation can be attributed to either the different measurement techniques used in the experiments or to the influence of external disturbances. Using the Orr-Sommerfeld equation, we obtained a critical Reynolds

number R_c=171 which is in good agreement with the theoretical results of Brown [14] and Cebeci and Stewartson [3] but is considerably less than the observed values. The value of the critical Reynolds number for stationary disturbances is significantly improved when the effects of Coriolis forces and streamline curvature are included. Our calculated critical Reynolds number of 287 for disturbances of this kind is in excellent agreement with the results obtained in [21] and [12] using hot wire techniques. Kobayashi et al [12] also performed a theoretical analysis in which some of the effects of Coriolis forces and streamline curvature were considered. They calculated a critical Reynolds number of 261.

In order to correlate transition using stability theory, one has to know the experimental location of the onset of transition. The transition Reynolds numbers usually given for experiments (see Table 1) are the locations where transition is complete. Gregory and Walker [22] showed that, for a slotted rotating disk, the transition region is composed of two subregions: (i) a vortex region and (ii) an intermediate turbulent region where the intermittancy factor γ varies from 0 to 1. Stability theory is only applicable up to the point where the first turbulence burst appears ($\gamma = 0$). Gregory and Walker obtained R = 505 and 524 for $\gamma = 0$ and $\gamma = 1$, respectively. Chin and Litt [23], using an electrochemical technique, observed that the transition was complete at R = 592. They also observed that the vortices start breaking down into turbulence at $R_T = 510$. We believe that this result should be taken as the relevant

location for the onset of transition for the purposes of comparison with stability theory. Further evidence that the initiation of transition occurs at $R_T \approx 510$ is provided by Kobayashi et al [12] who observe that the disturbances are non-linear at R = 500. Usually in boundary layer flows the non-linear region is relatively narrow so the onset of transition soon follows. Further, Federov et al [13] observed turbulent flow at R = 515. In the experiments of Ref. [21] turbulent spots first appeared at R = 513-526. On the basis of the evidence provided by these investigators [12,13,21-23] we take $R_T = 513$ as the location of the onset of transition for the purpose of applying the e^N correlation method.

Growth of Infinitesimal Disturbances

Disturbances of all frequencies may be present in natural transition. We follow the evolution of several different modes and the one which gives the highest integrated growth factor is used to correlate transition. Stationary disturbances were found to give the highest N factor for rotating disk flow over all positive real frequencies. Disturbances with negative phase velocities can give slightly higher N factors but they are of no consequence in the process of transition.

It was shown in [6] that the envelope method is a reliable tool for transition prediction in three dimensional flows. First, we report calculations using the Orr-Sommerfeld equation. The resulting N factors are compared with those of Cebeci and Stewartson [3] in Figure 1. It is evident that their method predicts N≈20 at transition (R = 513) while the present (envelope)

method gives N ≈ 22 at transition. Cebeci and Stewartson [3] used spatial stability theory and in order to remove arbitrariness among the parameters of equation (28), they imposed the condition

$$\frac{\partial \alpha_i}{\partial \beta_r} = 0 \tag{31}$$

where $\alpha_i = \mathrm{Im}(\alpha)$, $\beta_r = \mathrm{Re}(\beta)$. In order to simplify their computations, Cebeci and Stewartson assumed that the maximum growth rate at any $R>R_C$ is independent of the growth direction. We believe that had their growth rates been maximized over all possible growth directions their N factor at transition would be in better agreement with the present predictions using the Orr-Sommerfeld equation.

In Fig. 2 we plot calculated temporal growth rates (Im ω) for stationary vortices. It can be seen that the inclusion of streamline curvature and Coriolis forces have a significant stabilizing effect. Calculations with only Coriolis terms (as done by Lilly [15] for Ekman flow) were also made. These results indicate that streamline curvature effects must also be included in order to model properly the physical problem.

Since the instability is spatial in nature, we transform temporal growth rates to spatial growth rates σ using the group velocity transformation

$$\sigma = \frac{\mathrm{Im}(\omega)}{\mathrm{Re}(\omega_\alpha)} \tag{32}$$

The spatial growth rates are plotted in Figure 3. The effect of streamline curvature and Coriolis forces is found to

be very significant.

Integrated growth rate (N factor) results are presented in Figure 4. The present stability theory gives N ≈ 10.7 which is close to the value N = 9 for two dimensional flows and is in the range of values found for swept wings [6]. It is apparent that there is a very significant effect on the predicted transition N factor when the effects of Coriolis forces and streamline curvature are included. The resulting N factors are much lower than those obtained by conventional stability theory where only the Orr-Sommerfeld equation is solved.

Also presented in Figure 7 are experimental results from Ref. [21] for the N factor. The experimental amplification rate of the stationary vortices was determined by integrating the rms fluctuation spectrum in a narrow band centered on a frequency determined by the observed number of vortices, as described in [21]. Due to the problem with disk vibrations, the disturbance amplitude (A_0) at the minimum critical Reynolds number could not be measured with any certainty. It was assumed that $A_0 = 1$ and the resultant data were shifted at constant Reynolds number to match the theoretical growth curve. The data are seen to be in a fair agreement with the present theory over the range 400 <R<500. The significant deviation of the data for R<400 is attributed to disk vibrations. The falling off of the data for R>500 is due to the highly nonlinear nature of the flow in this region and breakdown to turbulence.

Although shifting the level of the data because of uncertainty in the value of A_0 can be questioned and the resultant

data can not be used to show conclusive support for the theory, the fact that the slope of the experimental curve ($\sigma = dN/dR$) matches the present theory in the range $400<R<500$ is very encouraging.

Orientation and Number of Vortices

In the envelope method we maximize growth rates $Im(\omega)$ for stationary vortices over all possible wave angles. We find that the vortex spirals make an angle of about 11.2° with the negative of the direction of disk rotation. This is within the range of the experimental value of $11\text{-}14^{\circ}$ [10-13]. The predicted angle varies very slowly with R.

It can be shown that the number of vortices is given by

$$n = \beta R \tag{33}$$

where β is defined in (15). Our calculations show that β remains almost constant (≈ 0.0698) so that n varies nearly linearly with R. The numerically predicted variation of number of stationary vortices is plotted in Figure 5 along with the experimental data [21]. The experimental results show that there are about 21 vortices at a Reynolds number of 294. The number of vortices increases radially and there appear about 29-31 vortices at $R \approx 513$. This radial increase in n is apparently due to the branching of individual vortices with increasing R. Although the data fall well below the theoretical curve at high Reynolds numbers, it does substantiate the overall trend predicted by the theory.

Previous investigators [10,12,13,25] have not suggested any direct correlation between the number of vortices and the

Reynolds numbers. A careful analysis of their data (Figure 5), however, shows that their results do not necessarily disagree with the present findings.

Parallel or Type II Instability

Lilly [15] presented numerical solutions of the Ekman layer problem and included the effect of Coriolis forces in his analysis. He found that at very low Reynolds numbers an instability mechanism exists whose disturbances are different from the stationary disturbances described previously. Lilly called this "parallel instability" and suggested that it is of viscous type since it vanishes at high Reynolds numbers. He found that the critical Reynolds number for these fast moving disturbances is 55 and the resulting modes are oriented at small negative angles. The orientation angle at the critical point is -23° which decreases in magnitude as the Reynolds number increases. A similar instability mechanism was detected in the experiments of Faller and Kaylor [16] (who called it a type II instability) and Tatro and Mollo-Christensen [17].

In our calculations, we also find travelling disturbances (f ~ 100 Hz relative to the disk) at Reynolds numbers much lower than the critical Reynolds number for stationary disturbances. The critical Reynolds number for travelling disturbances is calculated to be about 49. These disturbances appear to have characteristics similar to those reported by Lilly [15].

6. CONCLUSIONS

The growth of instabilities in the three-dimensional flow due to a rotating disk is studied using linear stability theory

including the effects of Coriolis forces and streamline curvature. Using the e^N analysis for transition prediction in these three dimensional boundary layers the N value is the order 11. Recent experiments [21] tend to support the theoretical prediction that the number of stationary vortices increases with R.

REFERENCES

1. Srokowski, A. J. and Orszag, S. A., "Mass Flow Requirements for LFC Wing Design", AIAA paper 77-1222.
2. Nayfeh, A. H., "Stability of Three-Dimensional Boundary Layers", AIAA J., Vol. 18, 1980, pp. 406-416.
3. Cebeci, T. and Stewartson, K., "On Stability and Transition in Three-Dimensional Flows", AIAA J., Vol. 13, 1980, pp. 398-405.
4. Smith, A.M.O. and Gamberoni, N., "Transition, Pressure Gradient, and Stability Theory", Report No. ES 26388, Douglas Aircraft Company, August 1956.
5. Hefner, J. N. and Bushnell, D. M., "Application of Stability Theory to Laminar Flow Control", AIAA Paper No. 79-1493.
6. Malik, M. R. and Orszag, S. A., "Comparison of Methods for Transition Prediction Using Three-Dimensional Stability Theory", AIAA Paper 80-1375.
7. Poll, D.I.A., "Some Aspects of the Flow Near a Swept Attachm, Line with Particular Reference to Boundary Layer Transition", C of A Report 7805. Cranfield Institute of Technology, Cranfield, August 1978.
8. von Karman, T., "Uber Laminare and Turbulente Reibung", Zeitschrift fur angewandte Mathematik und Mechanik, Vol. 20, pp. 241-253, 1940.
9. Smith, N. H., "Exploratory Investigation of Laminar Boundary Layer Oscillations on a Rotating Disk", N.A.C.A. Tech. Note No. 1227 (1947).
10. Gregory, N., Stuart, J. T. and Walker, W. S., "On the

Stability of Three-Dimensional Boundary Layers with Application to the Flow Due to a Rotating Disk", Philosophical Transactions of the Royal Society, London, Series A, 248, 1955, pp. 155-199.

11. Clarkson, M. H., Chin, S. C. and Shacter, P., "Flow Visualization of Inflexional Instabilities on a Rotating Disk", Paper No. 80-0279.

12. Kobayashi, R., Kohama, Y. and Takamadate, Ch., "Spiral Vortices in Boundary Layer Transition Regime on a Rotating Disk", Acta Mechanica, Vol. 35, 1980, pp. 71-82.

13. Fedorov, B. I., Plavnik, G. Z., Prokhorov, I. V. and Zhukhovitskii, L. G., "Transitional Flow Conditions on a Rotating Disk", J. Engineering Physics, Vol. 31, 1976, pp. 1448-1453.

14. Brown, W. E., "Numerical Calculation of the Stability of Cross Flow Profiles in Laminar Boundary Layers on a Rotating Disk and on a Swept-Back Wing and an Exact Calculation of the Stability of the Blasius Velocity Profile", Northrop Aircraft Report NAI-59-5, January 1959.

15. Lilly, D. K., "On the Instability of Ekman Boundary Flow", J. Atmospheric Sciences, Vol. 23, 1966, pp. 481-494.

16. Faller, A. J. and Kaylor, R. E., "Investigations of Stability and Transition in Rotating Boundary Layers", Ed. S. I. Pai, Dynamics of Fluids and Plasmas, Academic Press, N. Y., 1966, pp. 309-329.

17. Tatro, P. R. and Mollo-Christensen, E. L., "Experiments on Ekman Layer Instability", J. Fluid Mech., Vol. 28, 1967, pp. 531-543.

18. Orszag, S. A., "Accurate Solution of the Orr-Sommerfeld Stability Equation", J. Fluid Mech., Vol. 50, 1971, pp. 689-703.

19. Gottlieb, D. and Orszag, S. A., "Numerical Analysis of Spectral Methods", NSF-CBMS Monograph No. 26, Soc. Ind. and Appl. Math. (1977).

20. Wilkinson, J. H., "The Algebraic Eigenvalue Problem", Oxford (1965).

21. Malik, M. R., Wilkinson, S. P. and Orszag, S. A., "Instability and Transition in Rotating Disk Flow", to be published in AIAA J.

22. Gregory, N. and Walker, W. S., "Experiments on the Effect of Suction on the Flow Due to a Rotating Disk", J. Fluid Mech., Vol. 9, 1960, pp. 225-234.

23. Chin, D. and Litt, M., "An Electrochemical Study of Flow Instability on a Rotating Disk", J. Fluid Mech., Vol. 54, 1972, pp. 613-625.

24. Cobb, E. C. and Saunders, O. A., "Heat Transfer from a Rotating Disk", Proc. Roy. Soc., Series A 236, 1956, pp. 343-351.

25. Kitamura, O., "Experimental Investigation on Transition of the Boundary Layer Formed on a Rotating Disk (in Japanese)", M.S. Thesis, Dept. Mech. Eng., Hokkaido University, 1973.

TABLE 1. EXPERIMENTAL CRITICAL AND TRANSITION REYNOLDS NUMBERS FOR STATIONARY VORTEX FLOW

	Reynolds Number			
Investigators	Critical	Transition	Onset of Transition	Method of Investigation
Smith [9] (1947)	460	557	-	hot-wire probe
Gregory et al [10] (1955)	430	530	-	visual (China clay technique)
Cobb & Saunders [24] (1956)	447	490	-	heat transfer from the disk
Gregory & Walker [22] (1960)	367	524	505	acoustical slotted disk
Chin & Litt [23] (1972)	412	592	510	mass transfer coefficient using electro-chemical
Fedorov et al [13] (1976)	387	515	-	visual (Napthalene), acoustical
Clarkson et al [11] (1980)	532-621	562-680	-	visual (dye in water)
Kobayashi et al [12] (1980)	297	566	500 (non-linear)	hot wire probe
Malik et al [21]	294	-	513-526	hot wire probe

FIGURE CAPTIONS

FIGURE 1. Integrated growth factor using Orr-Sommerfeld equation

(a) Present calculations

(b) Cebeci and Stewartson [3]

FIGURE 2. Temporal growth rates for stationary vortices

(a) Orr-Sommerfeld equation

(b) Orr-Sommerfeld equation with Coriolis force effects included

(c) Orr-Sommerfeld equation with Coriolis force and streamline curvature effects included

FIGURE 3. Spatial growth rates for stationary vortices

(a) Orr-Sommerfeld equation

(b) Present theory

FIGURE 4. Integrated growth factor for stationary vortices

(a) Orr-Sommerfeld equation

(b) Present theory

FIGURE 5. Number of stationary vortices as a function of R.

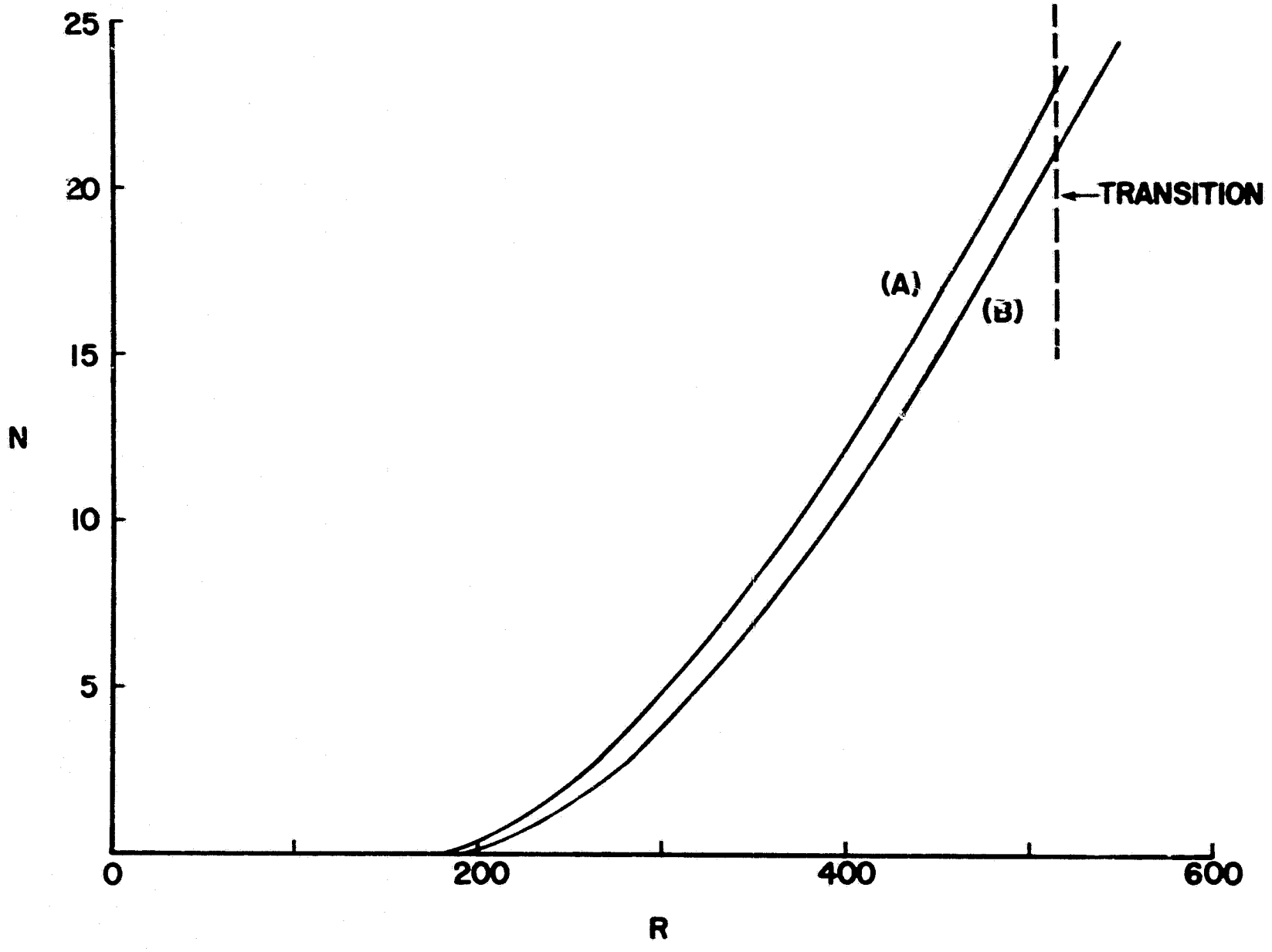

FIGURE 1

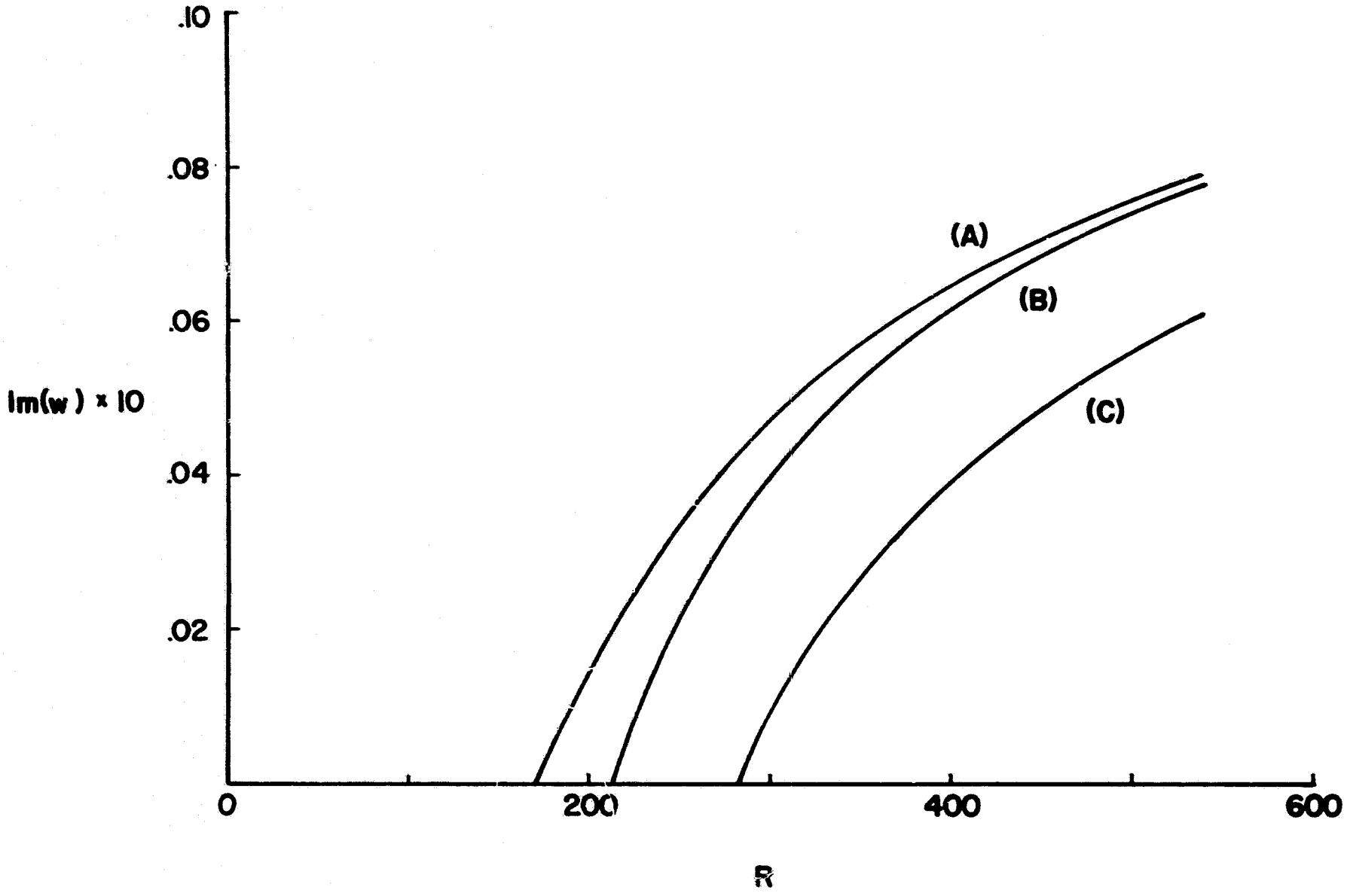

FIGURE 2

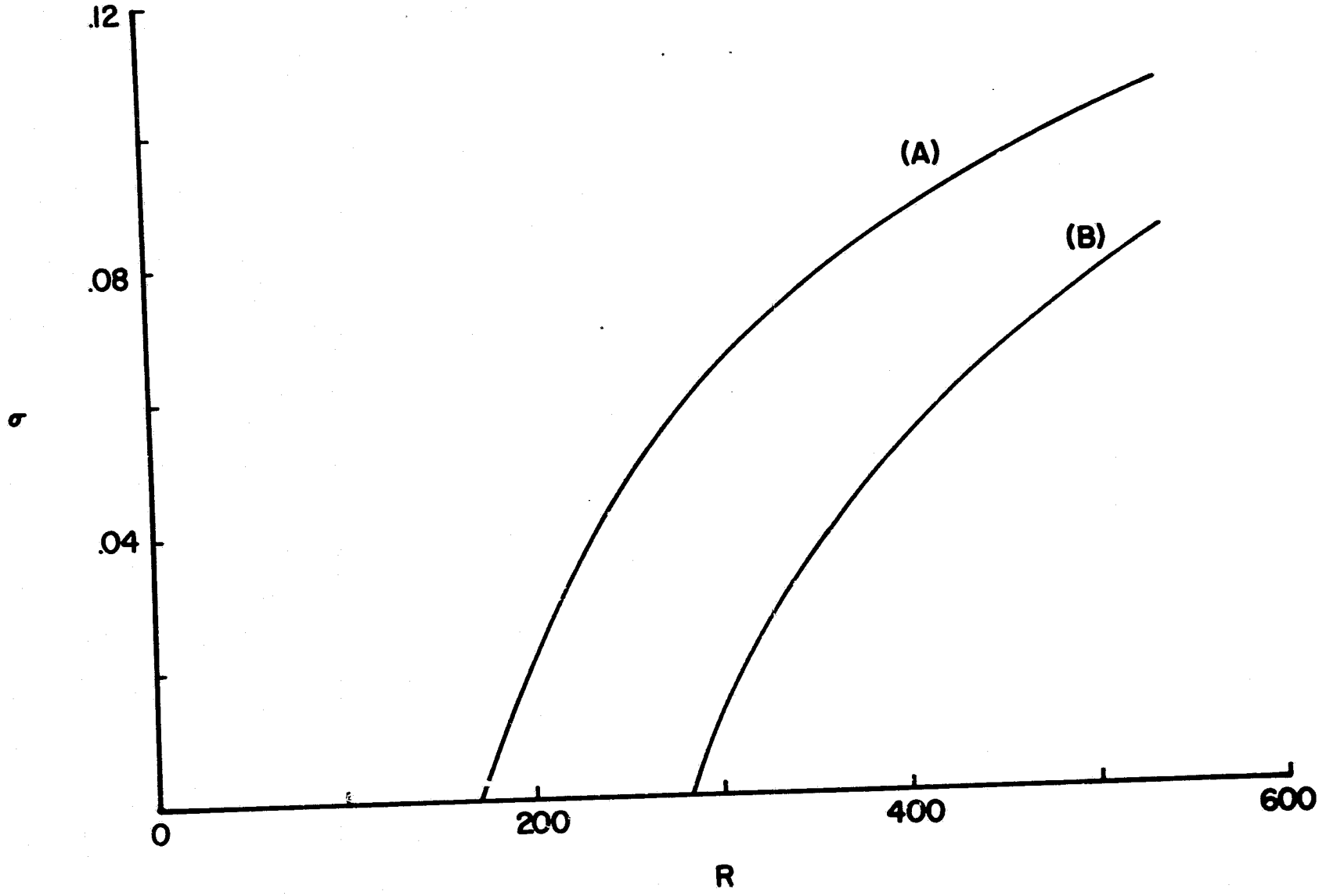

FIGURE 3

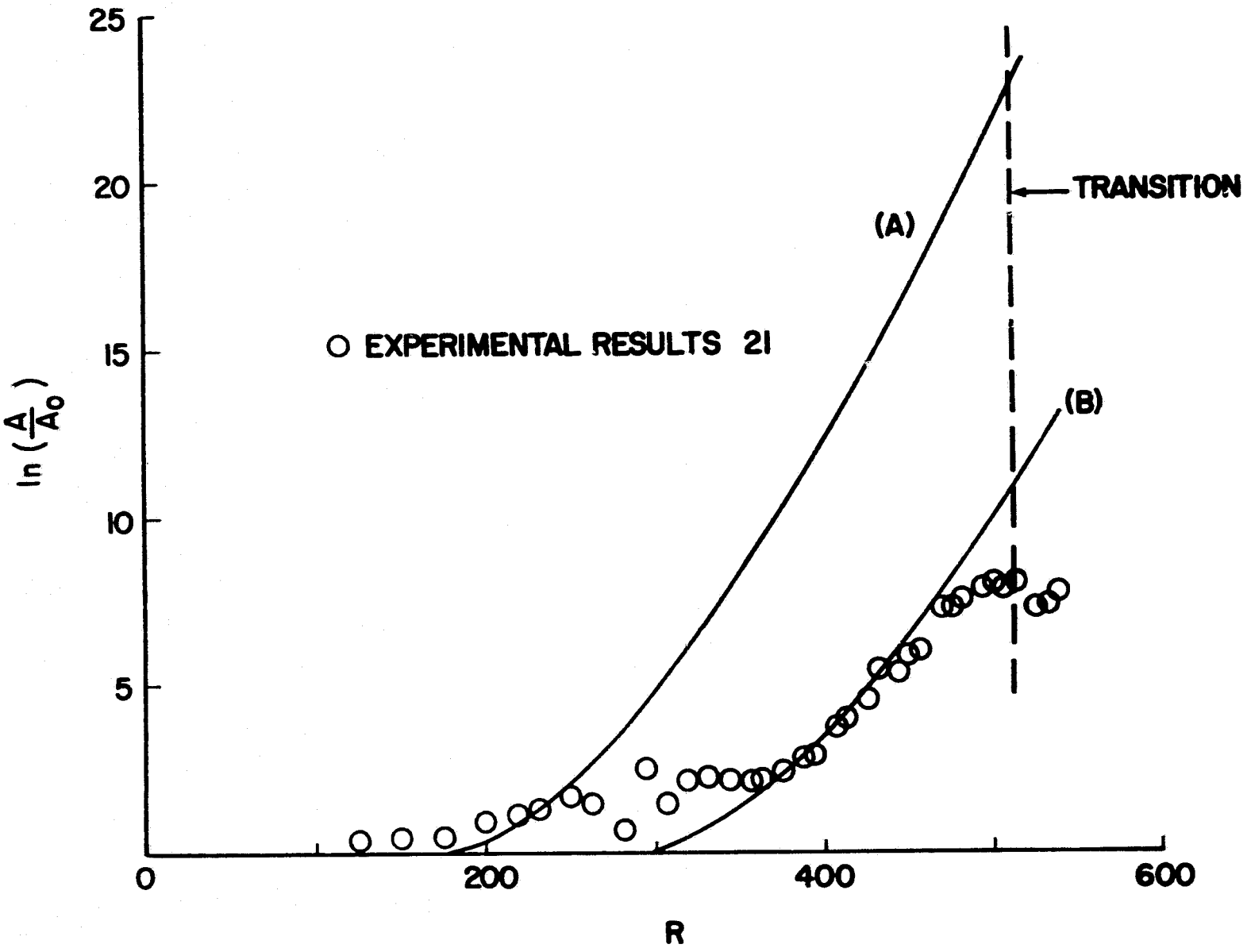
25
20
15
10
5
0
200
400
600
R
ln (A/Ao)
O EXPERIMENTAL RESULTS 21
(A)
(B)
TRANSITION

FIGURE 4

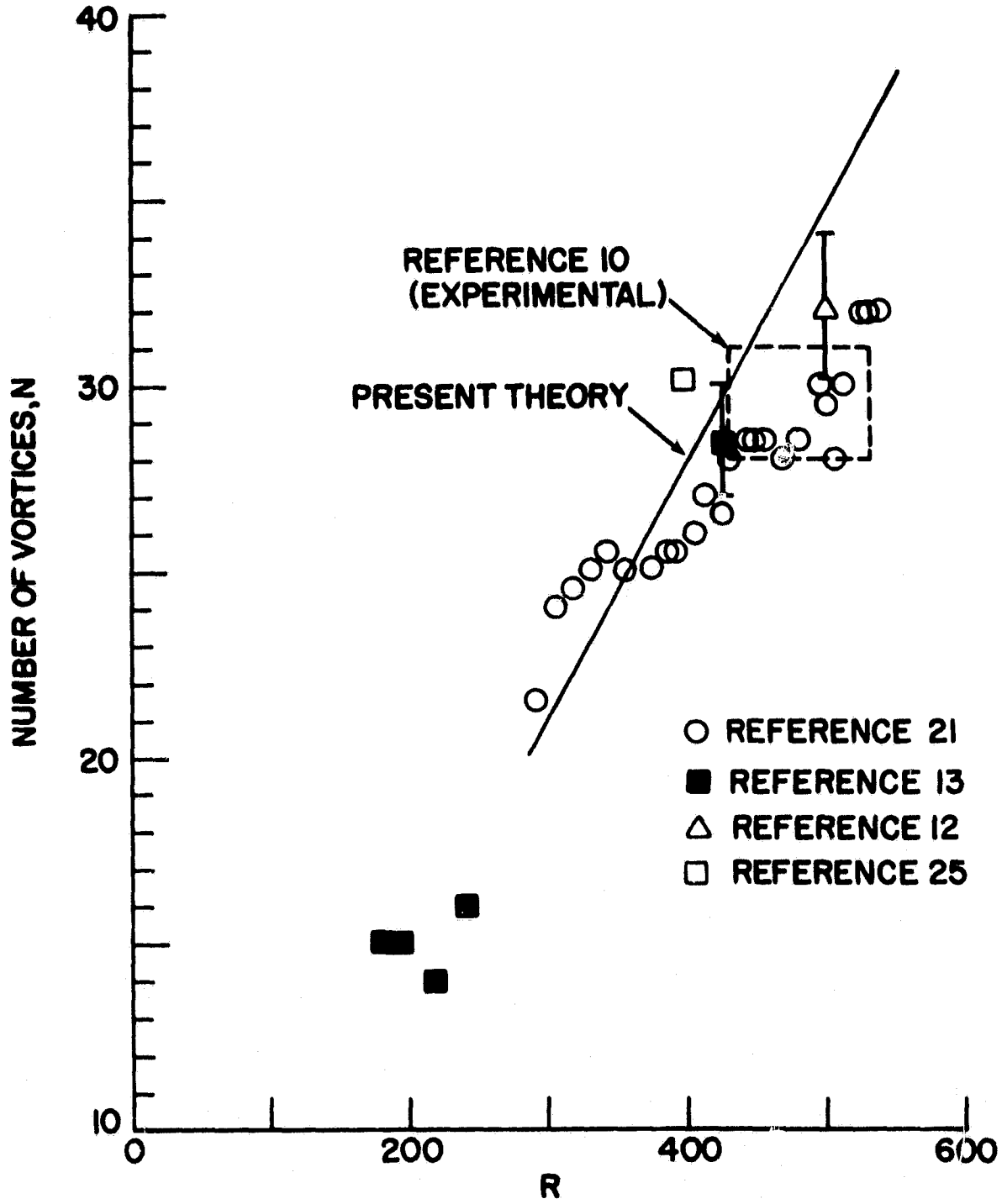
40
30
20
10
0
200
400
600
R
NUMBER OF VORTICES, N
REFERENCE 10
(EXPERIMENTAL)
PRESENT THEORY
REFERENCE 21
REFERENCE 13
REFERENCE 12
REFERENCE 25

FIGURE 5